Synthesis and structural characterization of adaptable shape-persistent building blocks

Charles Degenhardt III, David Brian Shortell, Richard D. Adams and Ken D. Shimizu*

Department of Chemistry and Biochemistry, University of South Carolina, Columbia, SC 29208 USA. E-mail: shimizu@mail.chem.sc.edu

Received (in Columbia, MO, USA) 8th March 2000, Accepted 5th April 2000

The rigid *syn*- and *anti*-atropisomers of diacids 1 and 2 were synthesized and assigned by symmetry-based methods and X-ray crystallography.

Rigid difunctional molecules are key components in synthetic molecular receptors and shape-persistent molecular polymers.[1,2] Reported herein are the syntheses and structures of two new diacid building blocks **1** and **2**. Both maintain highly rigid

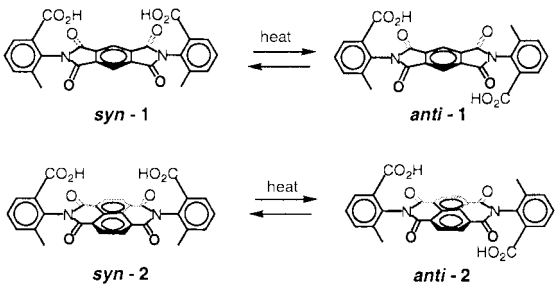

and coherent conformations due to aromatic components and restricted rotation about two linking N_{imide}–C_{aryl} bonds.[3] The resulting *syn*- and *anti*-atropisomers are stable at room temperature but interconvert on heating.

Diacids **1** and **2** were synthesized in high yields by condensation of the corresponding arylamine and aromatic dianhydrides (Scheme 1).[4] In each case, the presence of restricted rotation was immediately evident by the isolation of two spectroscopically similar molecules that interconverted on heating. The stable atropisomers were readily separated by flash chromatography and could be derivatized without isomerization. To further demonstrate their stability, the individual *syn*- and *anti*-isomers of diamides **3** and **4** were synthesized from the corresponding isomers of diacids **1** and **2**.

The rotational barrier of the C_{aryl}–N_{imide} bonds was measured in diamides **3** and **4**. Rotational barriers of $\Delta G^{\ddagger}$ = 29.4 kcal mol^{-1} ($t_{1/2}$ = 35 h at 77 °C) for **3** and $\Delta G^{\ddagger}$ = 34.0 kcal mol^{-1}

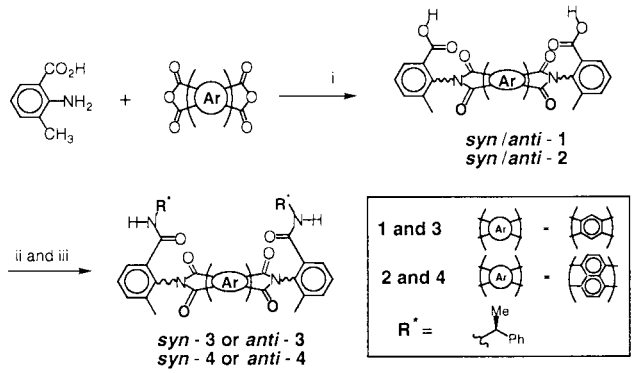

Scheme 1 *Reagents and conditions*: i, DMF, reflux, 8 h, (80% yield) or neat, *in vacuo*, 150 °C, 12 h, (95% yield); ii, oxalyl chloride, cat. DMF, CH_2Cl_2, reflux 2 h; iii, (*S*)-α-methylbenzylamine, triethylamine, CH_2Cl_2, 1 h, (70–80% yield for steps ii and iii).

($t_{1/2}$ = 4.1 h at 152 °C) for **4** were determined from the equilibration rates in DMSO. The higher rotational barrier of naphthalene diimide **4** appears to be due to increased steric effects in the six-membered cyclic imides. Molecular modeling calculations correctly predicted the magnitude and ordering of this trend.[5]

For diacids **1** and **2**, 1D and NOE NMR experiments could not lead to assignment of the atropisomers owing to their high symmetries. Instead, symmetry-based characterization methods were applied which efficiently identified the *syn*- and *anti*-isomers without the necessity of X-ray crystallography.[6] Derivatization of the diacids with a chiral auxiliary reduced the symmetry of the corresponding isomers in a predictable manner that yielded characteristic ^{1}H NMR spectra. This was achieved experimentally by reaction of the individual *syn*- and *anti*-isomers of the diacid chlorides of **1** and **2** with (*S*)-α-methylbenzylamine to yield the *syn*- and *anti*-isomers of diamides **3** and **4**. The chiral auxiliary accentuates the differences in symmetry of the *syn*- and *anti*-isomers and allowed assignment based on the chemical equivalence or inequivalence of the protons of the diimide spacer. For example, the two protons of the benzene diimide spacer in **3** are chemically equivalent in the *syn*-isomer and inequivalent in the *anti*-isomer (Fig. 1). A similar analysis of diamide **4** predicts that adjacent protons in *anti*-**4** and diagonal protons in *syn*-**4** are chemically equivalent. The corresponding ^{1}H NMR spectra of *anti*- and *syn*-**4** exhibited two singlets and two doublets, respectively.

Corroboration for the symmetry-based assignments was provided by polarity-based arguments and an X-ray crystal

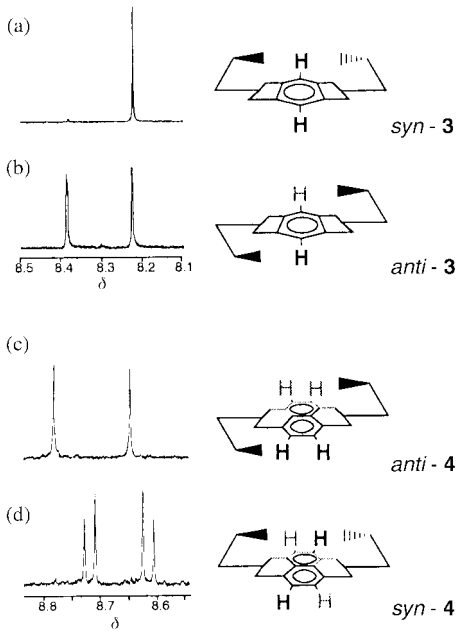

Fig. 1 Proton NMR spectra (DMSO-d_6, 400 MHz) of chiral diamides **3** and **4** and schematic representations showing the symmetry present in each rotamer; (a) *syn*-**3**, (b) *anti*-**3**, (c) *anti*-**4**, (d) *syn*-**4**.

DOI: 10.1039/b002085k

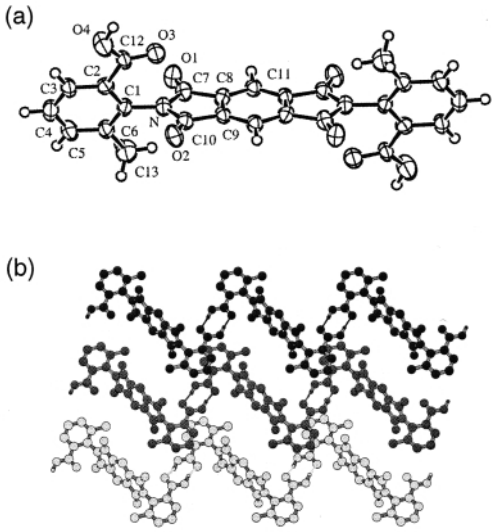

Fig. 2 (a) X-Ray structure of *anti*-**1** and (b) extended hydrogen-bonded ribbon structure of **1**. Solvent molecules and non-carboxylic acid hydrogens have been omitted for viewing clarity.

structure of *anti*-**1**. Initially, the atropisomers were tentatively identified based on polarity as measured by thin layer chromatography on silica gel. The *anti*-conformer was expected to be the less polar (higher R_f) owing to its inversion symmetry.[7] For all of the *N*,*N*′-diarylimide atropisomers examined thus far, the symmetry- and polarity-based assignments have been in agreement. In the case of diacid **1**, further evidence for the correct assignment was provided by an X-ray crystal structure [Fig. 2(a)] of the *anti*-isomer, which was crystallized from $MeCO_2H$–CH_2Cl_2.† The *anti*-configuration was immediately evident from the inversion symmetry of the space group ($P\bar{1}$) coupled with the small unit cell that contained approximately half of the atoms in diacid-**1**.

The structure also revealed interesting information about the molecular and extended structures. The positions of the non-hydrogen atoms of *anti*-**1** were well defined and revealed a structure with the *N*-aryl rings rotated 73° out of the plane of the diimide spacer. In the extended structure [Fig. 2(b)] *anti*-diacid **1** forms a hydrogen-bonded ribbon polymer with channels along the *a*-axis filled with disordered acetic acid dimers which was the source of the relatively high *R*-value for the structure.

This work was supported by grants from the NSF (DMR-9807470) and the Research Corporation (RI0081).

Notes and references

† *Crystal data for anti*-**2**: $C_{26}H_{16}N_2O_8{\cdot}2CH_3CO_2H$, M = 578.49, triclinic, space group $P\bar{1}$, a = 8.403(2), b = 11.995(3), c = 7.7872(2) Å, α = 98.41(2), β = 95.41(2), γ = 109.72(2)°, U = 722.5(4) A^3, T = 293 K, Z = 1, μ(Mo-Kα) = 0.106 mm^{-1}, 1444 observed reflections, R = 0.105, R_w = 0.176. The high R-factor is a consequence of disorder in the cocrystallized acetic acid molecules.

CCDC 182/1605. See http://www.rsc.org/suppdata/cc/b0/b002085k/ for crystallographic files in .cif format.

1 J.-M. Lehn, *Supramolecular Chemistry: Concepts and Perspectives*, VCH, New York, 1995; F. Vögtle, *Supramolecular Chemistry*, John Wiley and Son, 1993.

2 J. S. Moore, *Acc. Chem. Res.*, 1997, **30**, 402; S. Hoger, *J. Polym. Sci. Polym. Chem.*, 1999, **37**, 2685; A. J. Berresheim, M. Muller and K. Mullen, *Chem. Rev.*, 1999, **99**, 1747.

3 K. D. Shimizu, T. M. Dewey and J. Rebek Jr., *J. Am. Chem. Soc.*, 1994, **116**, 5145; J. Rebek Jr., *Angew. Chem., Int. Ed. Engl.*, 1990, **29**, 245.

4 All new compounds reported here were fully characterized on the basis of their spectral (UV, IR, ^{1}H and ^{13}C NMR, MS). Selected data for *anti*-**1**: IR (KBr) 3425, 2976, 1781, 1686 cm^{-1}; ^{1}H NMR (400 MHz, DMSO-d_6) δ 8.49 (s, 2H), 7.94 (dd, J 6.6, 1.2 Hz, 2H), 7.70 (d, J 7.1 Hz, 2H), 7.58 (t, J 7.7 Hz, 2H), 2.26 (s, 6H). ^{13}C NMR (100 MHz, DMSO-d_6) δ 165.78, 165.15, 138.54, 137.14, 134.77, 129.86, 129.49, 128.95, 128.8, 118.46, 17.35; HRMS (FAB, NBA) calc. for $C_{26}H_{16}N_2O_8$ (M + H) *m/z* 485.0985, obs. 485.0976. Anal. Calc. for $C_{26}H_{16}N_2O_8{\cdot}H_2O$: C, 60.00; H, 3.87; N, 5.38. Found: C, 60.14; H, 3.64; N, 5.39%. For *syn*-**1**: IR (KBr) 3425, 1780, 1729, 1690 cm^{-1}; ^{1}H NMR (400 MHz, DMSO-d_6) δ 8.53 (s, 2H), 7.94 (dd, J 5.5, 1.5 Hz, 2H), 7.71 (d, J 7.5 Hz, 2H), 7.59 (t, J 7.7 Hz, 2H), 2.25 (s, 6H). ^{13}C NMR (100 MHz, DMSO-d_6) δ 165.77, 165.12, 138.37, 137.09, 134.78, 129.83, 129.55, 129.04, 128.88, 118.65, 17.26; HRMS (FAB, NBA) calc. for $C_{26}H_{16}N_2O_8$ (M + H) *m/z* 485.0985, obs. 485.0995. Anal.Calc. for $C_{26}H_{16}N_2O_8$: C, 64.47; H, 3.33; N, 5.78. Found: C, 64.21; H, 3.55; N, 5.85%. For *syn*-**2**: IR (KBr) 3200, 1715, 1664, 1582 cm^{-1}; ^{1}H NMR (400 MHz, DMSO-d_6) δ 12.91 (br s, 2H), 8.77 (s, 4H), 7.98 (d, J 6.8 Hz, 2H), 7.70 (d, J 6.9 Hz, 2H), 7.55 (t, J 6.7 Hz, 2H), 2.21 (s, 6H). ^{13}C NMR (100 MHz, DMSO-d_6) δ 167.49, 164.02, 139.37, 136.52, 136.10, 132.53, 130.92, 130.50, 129.94, 128.62, 128.27, 18.90; HRMS (FAB, NBA) calc. for $C_{30}H_{18}N_2O_8$ (M + H) *m/z* 535.1141, obs. 535.1147. For *anti*-**2**: IR (KBr) 3199, 1713, 1676, 1580 cm^{-1}; ^{1}H NMR (400 MHz, DMSO-d_6) δ 12.42 (br s, 2H), 8.79 (s, 4H), 7.98 (d, J 7.5 Hz, 2H), 7.71 (d, J 7.2 Hz, 2H), 7.56 (t, J 7.6 Hz, 2H), 2.21 (s, 6H). ^{13}C NMR (100 MHz, DMSO-d_6) δ 165.68, 162.21, 137.41, 134.77, 134.26, 130.95, 129.25, 128.81, 128.21, 126.76, 126.37, 17.06; HRMS (FAB, NBA) calc. for $C_{30}H_{18}N_2O_8$ (M + H) *m/z* 535.1141, obs. 535.1144.

5 The barriers of rotation were calculated using MM2 as implemented in MacroModel v5.5 (F. Mohamadi, N. G. J. Richards, W. C. Cuida, R. Liskamp, M. Lipton, C. Caufield, G. Chang, T. Hendrickson and W. C. Still, *J. Comput. Chem.*, 1990, **11**, 440). The rotational barrier varied greatly with the step angle of the dihedral driver. Accurate values were attained only for small step angles of < 1°. Larger step angles would jump over the barrier and predict considerably smaller rotational barriers.

6 E. L. Eliel and S. H. Wilen, *Stereochemistry of Organic Compounds*, John Wiley & Sons, New York, 1994, pp. 669–670.

7 G. M. Sanders, M. Van Dijk, B. M. Machiels and A. van Veldhuizen, *J. Org. Chem.*, 1991, **56**, 1301.